Deciphering ^{98}Nb β decay with the Modular Total Absorption Spectrometer at ORNL

B. C. Rasco,[1,*] K. P. Rykaczewski,[1] A. Fijałkowska,[2,3] M. Karny,[2,4] M. Wolińska-Cichocka,[5,1,4] R. K. Grzywacz,[3,1,4] D. W. Stracener,[1] E. F. Zganjar,[6] J. C. Batchelder,[7,4] J. C. Blackmon,[6] N. T. Brewer,[4,1,3] M. P. Cooper,[3] K. C. Goetz,[8,3] J. W. Johnson,[1,†] T. King,[1] A. Laminack,[1] J. T. Matta,[1] K. Miernik,[2] M. Madurga,[3] D. Miller,[3,‡] M. M. Rajabali,[9] T. Ruland,[6] P. Shuai,[1,3,4,10] M. Stepaniuk,[2] and J. Winger[11]

[1]*Physics Division, Oak Ridge National Laboratory, Oak Ridge, Tennessee 37831, USA*
[2]*Faculty of Physics, University of Warsaw, Pasteura 5, PL-02-093 Warszawa, Poland*
[3]*Department of Physics and Astronomy, University of Tennessee, Knoxville, Tennessee 37966, USA*
[4]*JINPA, Oak Ridge National Laboratory, Oak Ridge, Tennessee 37831, USA*
[5]*Heavy Ion Laboratory, University of Warsaw, PL-02-093 Warszawa, Poland*
[6]*Department of Physics and Astronomy, Louisiana State University, Baton Rouge, Louisiana 70803, USA*
[7]*Department of Nuclear Engineering, University of California, Berkeley, Berkeley, California 94720, USA*
[8]*CIRE Bredesen Center, University of Tennessee, Knoxville, Tennessee 37966, USA*
[9]*Physics Department, Tennessee Technological University, Cookeville, Tennessee 38505, USA*
[10]*Institute of Modern Physics, Chinese Academy of Sciences, Lanzhou 730000, China*
[11]*Department of Physics and Astronomy, University of Mississippi, Starkville, Mississippi 39762, USA*

(Received 2 February 2022; accepted 2 May 2022; published 3 June 2022)

Background: An assessment done under the auspices of the Organization for Economic Co-operation and Developement Nuclear Energy Agency (OECD-NEA) in 2007 suggested that the β decays of many abundantly produced fission products in nuclear reactors may be incomplete. In this assessment, the fission product ^{98}Nb was assigned the highest priority for study by total absorption spectroscopy due to its large cumulative fission branching fraction and because the β-decay data from several experiments are discrepant.
Purpose: To obtain the complete β-decay feeding pattern of ^{98}Nb and determine the impact on the average γ energy per ^{98}Nb β decay and $\bar{\nu}_e$ emission calculations. The complete ^{98}Nb β-decay feeding pattern includes ground-state to ground-state β feeding and direct β feeding to the 0^+ first-excited state (both have no associated γ rays), and the ground-state to excited-state β transitions followed by γ transitions to the ground state of the daughter nucleus, ^{98}Mo.
Method: The complete β-decay intensities of ^{98}Nb were measured with the Modular Total Absorption Spectrometer at Oak Ridge National Laboratory (ORNL). The ^{98}Nb was produced by the β decay of mass 98 fission fragments at ORNL's On-Line Test Facility (OLTF) using proton-induced fission of ^{238}U.
Results: We find that changes to the current ENSDF assessment of ^{98}Nb β-decay intensity are required. We report improved uncertainties for the β-decay feeding values and report new β feedings to high-energy levels in ^{98}Mo.
Conclusions: A more complete ^{98}Nb β-feeding pattern with improved accuracy and precision is offered. The impacts of the measured changes to the ^{98}Nb β-feeding pattern on both reactor decay heat calculations and predicted detection rates of reactor $\bar{\nu}_e$ are presented. The Modular Total Absorption Spectrometer measurements of ^{98}Nb demonstrate the importance of reexamining and remeasuring complex β-decaying fission products with total absorption spectroscopy, including nuclei very near β stability.

DOI: 10.1103/PhysRevC.105.064301

I. INTRODUCTION

Accurate and precise understanding of β-decay feedings influences many different areas of physics, from applied research to fundamental physics. In the mid-1970s, a possible systematic one-direction bias for β-decay feedings to high energy levels with high level density measured with low-efficiency detectors was identified [1], and this systematic bias is referred to as the pandemonium effect. The pandemonium effect impacts incomplete β-decay schemes by raising the average γ energy and lowering the average leptonic (β^- and $\bar{\nu}_e$) energy per decay. But the pandemonium-effect bias is not the only challenge that affects current β-decay data; there are other possible β-decay branches that are experimentally difficult to measure. Directly measuring the ground-state to ground-state feeding is challenging and more often than not it

*rascobc@ornl.gov
†Deceased.
‡Present Address: MKS Instruments, Inc., Rochester, NY 14623, USA.

is not measured at all. Many older experiments also had limited data acquisition systems with much lower total number of bits, which places an upper limit on the γ-ray energy that is measured, or used two separate experiments, one to measure lower energy γ rays and one with different gain to measure higher energy γ rays. Low-efficiency detectors also require longer experimental run times to identify γ-γ correlations, not to mention γ-γ-γ, γ-γ-γ-γ, and higher correlations. Unlike the pandemonium effect, these other effects are not systematically one-direction corrections for average γ and lepton energies. In the end, the only way to find accurate and precise β-feeding patterns needed for reactor decay heat and reactor $\bar{\nu}_e$ calculations is to measure each β-decay component.

The ^{98}Nb β-decay feeding pattern is important to properly understand because of its large cumulative fission yield for the main reactor fuels, such as ^{235}U (5.75(132)%) and ^{239}Pu (5.9(13)%) [2], even though it has a small direct fission yield. Because of its large cumulative fission yields, its relatively large Q_β of 4591(5) keV, conflicting experimental data, and the reasonably large discovery window of 1983(5) keV (the discovery window is the difference in energy between the highest known level fed by β decay and the Q_β), ^{98}Nb was identified as a priority 1 fission product to study using the total absorption technique [3]. This assigned high priority emphasizes the importance of the ^{98}Nb β-decay feeding pattern on both reactor decay heat [3] and reactor-$\bar{\nu}_e$ calculations [4–6]. ^{98}Nb also potentially impacts the reactor-$\bar{\nu}_e$ spectral fine structure [7].

There are many reported total absorption spectroscopy experiments that result in improved β-feeding patterns, and a few selected results are offered here [8–16]. The present results are the first reported measurements of ^{98}Nb using the total absorption spectroscopy experimental technique.

The history of ^{98}Nb β-decay experimental results spans several decades and includes conflicting results. ^{98}Nb is one β decay away from stability and has been studied multiple times with different experimental setups [17–20]. The β-decay results from many of the experiments are in disagreement. The current ENSDF decay scheme is shown in Fig. 1.

The experimental disagreements originate from several challenging factors measuring ^{98}Nb β decay. The first challenge is that the first-excited state in the even-even daughter nucleus ^{98}Mo is a 735-keV 0^+ level (hereafter referred to as the 0_2^+ level). This level decays to the ground state via $E0$ conversion electrons only, no γ rays to the ground state are created, and its energy is too low to decay via $E0$ pair production. A second challenge is that the half-life of ^{98}Nb ($T_{1/2} = 2.86(6)$ s) is much shorter than its parent ^{98}Zr ($T_{1/2} = 30.7(4)$ s), and is therefore in β-decay equilibrium with its parent. In most experimental setups, including the present setup, separating these two β-decay components using their half-lives is not possible unless an assumption is made about one or the other decay patterns. A third challenge is that there is a long-lived isomer of 51.1 min that is populated with differing fractions depending on the ^{98}Nb production method used. This can be suppressed through the time structure of each experimental setup, though this was not possible in all previous experimental setups. The last challenge is related to the various possible ^{98}Nb production methods, each of which have different forms of contamination that can make identifying and separating the ^{98}Nb β decays nontrivial. Each of these challenges are discussed in the present paper.

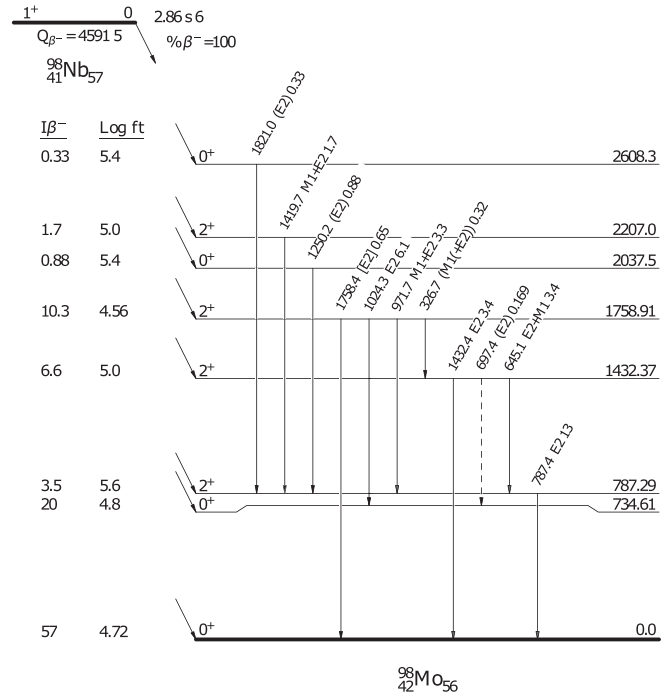

FIG. 1. The ^{98}Nb decay scheme. There is no γ ray from the decay of the 735-keV level since this is an E0 $0^+ \rightarrow 0^+$ transition. Image modified from Ref. [21].

II. EXPERIMENTAL OVERVIEW

Oak Ridge National Laboratory's Modular Total Absorption Spectrometer (MTAS) was used to measure ^{98}Nb β decay. MTAS is a one-ton modular NaI(Tl)-based total absorption spectrometer array that is segmented into 19 hexagonal modules of dimension 53.3 cm × 17.6 cm × 20.3 cm (21 inches × 7 inches × 8 inches) inches each [22]. The center module has a 63.5 mm (2.5-inch) through hole, where the activity is placed for measurement. In the heart of MTAS are two 1 mm × 40 mm × 60 mm silicon detectors with seven segments each. The individual silicon strips are normally only used as a β trigger and to position the activity in the center of the silicon strips which are centered in MTAS. For the present ^{98}Nb β decay, they are useful for isolating conversion electrons and hence the direct feeding to the 0_2^+ level in ^{98}Mo.

A motorized tape control system (MTC) is used to consistently transport the activity into the center of MTAS, which prevents the buildup of long-lived activities inside MTAS. Ions were implanted onto the magnetic tape outside of MTAS and then transported into MTAS. The implantation point was monitored by an HPGe detector to identify the beam elements by individual γ-ray energies and relative γ-ray intensities. Further details about the general MTAS experimental setup can be found in Refs. [22–24].

For this experiment, ^{98}Nb nuclei were not extracted directly from a positive ion source at the Holifield Radioactive

Ion Beam Facility at Oak Ridge National Laboratory. They were created as the daughters of nuclei that were extracted from the source. For mass 98, ^{98}Rb and ^{98}Sr ions were extracted from the source, with a mass resolution of $M/\Delta M = 600$. The extracted mass 98 nuclei then eventually β decay to ^{98}Zr and ^{98}Nb. The ^{98}Rb and ^{98}Sr were extracted from the positive ion source [25]. Based on the cumulative fission yields, it is expected that the ^{98}Rb production is at least 100 times less than the ^{98}Sr production [26], but Sr is much less efficiently extracted from the source than Rb. The competition between production in and extraction from the source is important to consider when comparing with certain previous ^{98}Nb experimental results [20].

In order to focus on the ^{98}Nb β decay, the tape movement was set to a cycle time with beam implanting on the tape for 60 s, the tape was moved into MTAS over 1 s, and the measurement was for 220 s, leading to a total cycle time of 281 s. For the extracted MTAS energy spectrum analyzed in this paper, a further offline time cut between 90 and 120 s in the total tape cycle are used; this is equivalent to a cut of 29 to 59 s of the measurement cycle. This cycle time along with the further offline time cuts minimizes the short-lived mass 97 and mass 98 contaminants. Long-lived mass 97 contaminants were minimally produced and their activities are naturally suppressed by their long half-lives. No γ-ray lines other than those from mass 97 and 98 nuclei were identified in the HPGe detectors.

The nuclei ^{98}Nb and ^{98}Zr are in β-decay equilibrium since the ^{98}Zr half-life, $T_{1/2} = 30.7(4)$ s, is much longer than the ^{98}Nb half-life, $T_{1/2} = 2.86(6)$ s. Because these two decays are in equilibrium, they cannot be separated. This leads to both ^{98}Nb and ^{98}Zr activities in the measured data. Because ^{98}Zr β decays 100% of the time to the ^{98}Nb ground state [19] and ^{98}Zr has much lower Q_β value, $Q_\beta = 2243(10)$ keV, the impact of the parent decay on measurement of the daughter decay is greatly reduced. Additional details are provided below.

The long-lived ^{98m}Nb 84-keV isomer of 51.1 min is assumed to be only very weakly populated from ^{98}Zr β decay. This assumption is based on the large tentative spin difference of the two nuclei, 0^+ (^{98}Zr) versus (5^+) (^{98m}Nb), and that ^{98}Zr β decays 100% of the time to the ^{98}Nb ground state [19]. If the ^{98m}Nb isomer is populated at all from ^{98}Zr β decay, its activity would additionally be suppressed by a factor of 100 due to its long half-life and our short measurement time cut.

There are many components of the ^{98}Nb β-decay nuclear puzzle, and the modularity of the Modular Total Absorption Spectrometer and the segmentation of the silicon β-trigger detectors can disentangle this.

III. SIMULATED ^{98}Nb ENSDF DATA VERSUS MTAS DATA

As mentioned previously, other than for the half-life calculations, the MTAS data used are from 90 to 120 s in each total tape cycle. This leads to approximately 100 000 ^{98}Nb β decays in MTAS. Data from the last 30 s of the tape cycle was used to subtract possible long-lived backgrounds. Additionally there is a minor background from background coincidence events, where a background event occurs within the coincidence time window of a β-trigger event [14,27].

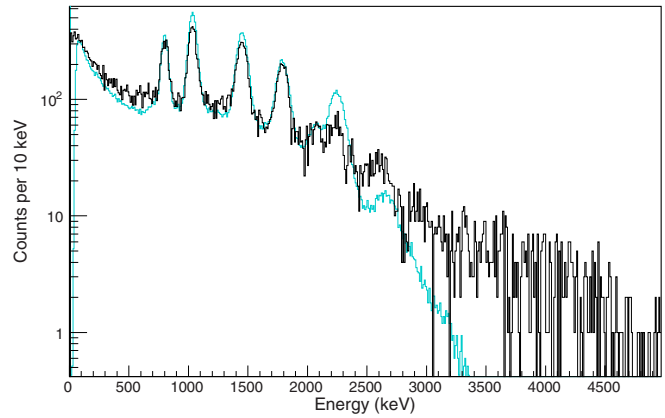

FIG. 2. The MTAS ^{98}Nb background subtracted data (black) compared to the simulated ENSDF data (cyan). There are clear differences in the two histograms. The spectra are normalized from 200 to 4500 keV. Slight excesses in the ENSDF feeding are seen in a few peaks and a large excess of the 2207-keV peak, while the low-energy spectrum is underestimated slightly. Additionally there is feeding detected in MTAS above the highest feed level in ENSDF at 2608 keV. These simple observations are indicative of the ground-state feeding being slightly underestimated and the feeding to higher levels being overestimated. There is likely new feeding above 2.6 MeV, possibly all the way to the Q_β energy limit.

The total MTAS data minus the various background components compared with the simulated ENSDF data is shown in Fig. 2. The ENSDF decay scheme is shown in Fig. 1. In Figure 2 there are differences at low energy that are likely from the ground-state 0^+_1 and first-excited 0^+_2 state feedings being underestimated in the current ENSDF data and there is possibly a small amount of additional β feeding at energies above the last known β-fed level at 2608 keV. These general interpretations are mostly born out in the full analysis, which is presented below.

IV. EXTRACTED HALF-LIFE

The extracted half-life from the MTAS data for the combined ^{98}Nb and ^{98}Zr β decays is $T_{1/2} = 30.8(20)$ s, in agreement with the ENSDF value for ^{98}Zr of $T_{1/2} = 30.7(4)$ s. Measuring the parent half-life is expected, since ^{98}Nb is in β-decay equilibrium with ^{98}Zr. The half-life is extracted from the total measurement portion of the cycle time of 220 s. The uncertainty is dominated by varying the endpoints of the fit of a single exponential with a flat background.

V. FITTING THE TOTAL MTAS ^{98}Nb ENERGY SPECTRUM

The results of fitting the total MTAS energy spectrum along with fitting of the energy spectra in the center module versus the total and individual inner, middle, and outer modules versus the total (for all of the major level energies) are shown in Fig. 3. This fitting technique is described in Ref. [14]. There are several comments about the data and the interpretation of the fit shown in Fig. 3. First, there are new levels identified above the previous highest β-fed level (2608 keV) in ENSDF. Second, the fit to the ground state (0^+_1) and the first-excited

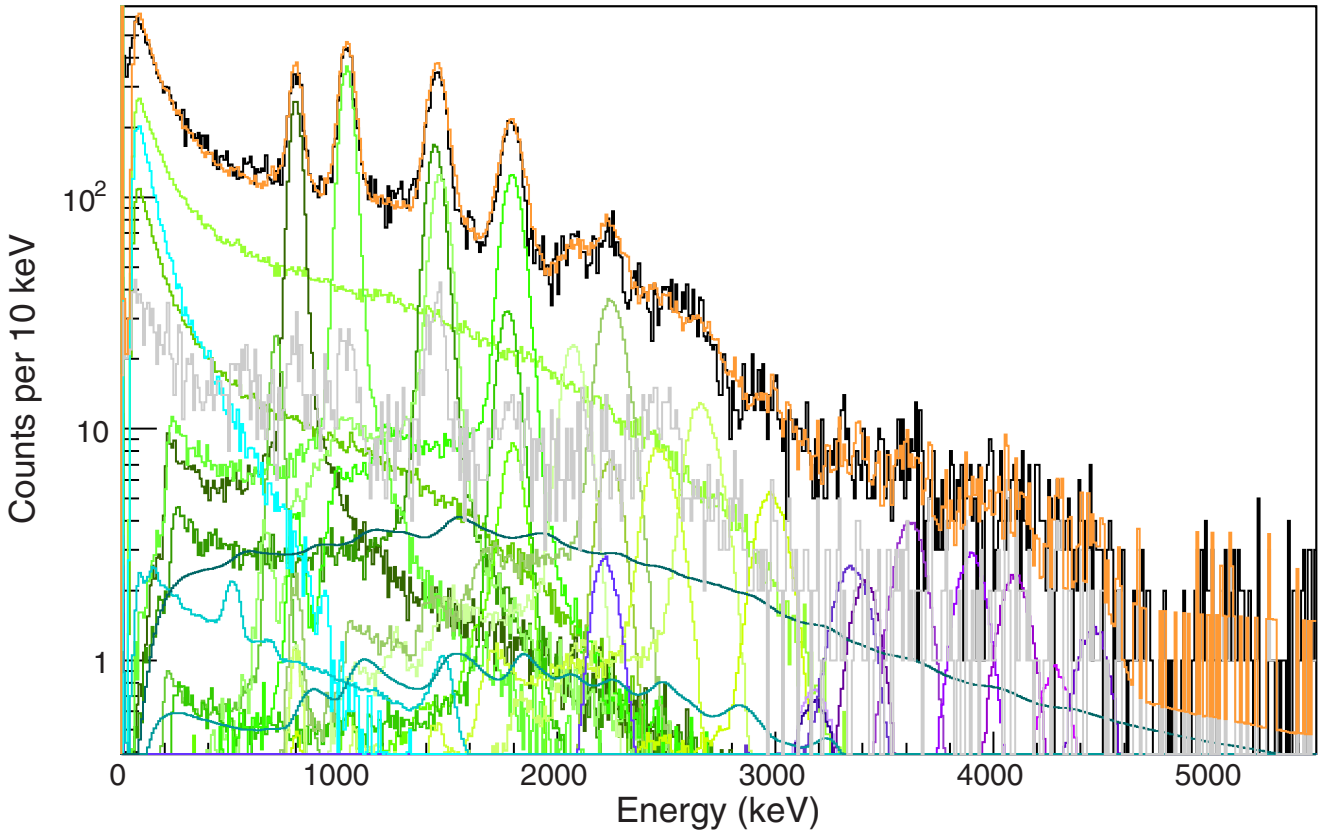

FIG. 3. Shown are the fit response functions decay paths by decay path (multicolored), the sum of all the fit components (orange), and the raw time-gated MTAS ^{98}Nb data (black). The ^{98}Zr decays (cyan), background coincidence (dark green), and the late-time gate component (gray) are shown. The late-time gate component contains some ^{98}Nb as well as a long lived background component. Both are likely there since the peak heights are different in the late cut and the early cut. The late background is normalized by measurement time.

state (0^+_2) are anticorrelated, because their signals in MTAS (response functions) are similar. A few comments on Fig. 2 are warranted. These comments concern interpretations of β decays to and through the 735-keV 0^+_2 level in ^{98}Mo. The peak at 1024 keV in Fig. 2 comes from the decay of 1759-keV level that decays through the 0^+_2 state, where the conversion electron is not detected in MTAS. The intensity from this peak is attributed to the 1759-keV level, but the intensity of this individual γ ray can be used to normalize the direct β feeding to the 0^+_2 level.

The new levels above the previously assumed highest level fed are identified with small statistics. These decays are identified with ^{98}Nb β decay via a measured half-life for events with energy above 2800 keV and less than approximately 4400 keV. A half-life of $T_{1/2} = 34(4)$ s for these levels is obtained. This uncertainty reflects the low number of statistics in the energy region. These additional levels are not part of the background coincidence spectra, as the energy spectrum from this type of background coincidence has a different spectral shape [14,27] than what is in the MTAS data. There are not enough counts of the decays from these new levels to identify the individual γ rays from these levels so it is assumed that they decay through the other known levels. The larger relative uncertainty in the β feeding to these levels reflects the uncertainty in the γ-ray multiplicity from these levels [28].

The basic component for fitting the MTAS energy spectrum is called a response function. There is a particular response function for each β-decay component (decay path) considered, such as the ground-state to ground-state transition and for each group of β particles and γ rays for the ^{98}Nb β decay. The dominant response functions are shown in Fig. 3. The response functions of the ground 0^+_1 state and the first-excited 0^+_2 state are very similar. This similarity of response functions implies the fit results are highly anticorrelated while the sum of the β-feeding intensity to these two levels is nearly constant. This is a generalization of one of Greenwood's conclusions about uncertainties in total absorption experiments, "I_β values assigned to adjacent levels are generally highly and negatively correlated", p. 538 [29]. I_β values assigned to *decay paths* with *similar response functions* are highly and negatively correlated. This anticorrelation is important to keep in mind when extracting the β feeding to the 0^+_2 735-keV level.

Since the ^{98}Nb β decay is in equilibrium with its parent, the β decay of ^{98}Zr is inseparable from ^{98}Nb. In order to account for the ^{98}Zr β-decay component, the number of ^{98}Zr β decays is normalized using the Bateman equation with a technique described in Ref. [27]. In the present case, the impact of the uncertainty from the Bateman equation normalization in minimized. This reduced impact is due to the

much lower efficiency of MTAS to detect β particles from the lower ^{98}Zr Q_β than from the higher energy (on average) β particles from ^{98}Nb. Since the Q_β for ^{98}Zr is much smaller, the efficiency with which a ^{98}Zr β decay to the ground state of ^{98}Nb deposits energy in MTAS is much lower. Based on simulations, the difference in Q_β values result in a β-triggered MTAS detection efficiency for the ^{98}Zr ground-state feeding of 3.2(3)% while for ^{98}Nb this efficiency is 20.0(5)%. This lower efficiency results in over six times less ^{98}Zr ground-state β decays depositing energy in MTAS than for ^{98}Nb ground-state to ground-state β decays. Due to this suppression in detected ^{98}Zr activity, the impact of the ^{98}Zr ground-state β decays on the ^{98}Nb ground-state uncertainty is not a large uncertainty. A bigger challenge is disentangling the direct β feeding to the 0^+_2 735-keV state in ^{98}Mo. Due to the modularity of both MTAS and the silicon detectors used for a β trigger, this decay component can be isolated.

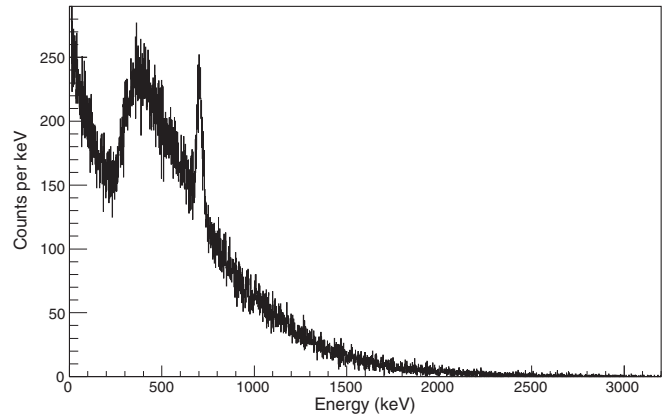

FIG. 4. Single silicon strip energy spectrum. There are a total of 14 silicon strips in the MTAS β-trigger detectors. The conversion electron peak is identifiable as the sharp peak just above 700 keV.

VI. EXTRACTING THE 0^+_2 STATE FEEDING

^{98}Nb presents a challenge for total absorption spectroscopy because the MTAS response functions to the first-excited 0^+_2 735-keV state and the ground-state 0^+_1 feeding are similar. Due to the similarity of the 0^+_1 and 0^+_2 response functions, for the full MTAS fit of these two decay paths are anticorrelated. This implies that the sum of the extracted β-feeding intensities for these two decay paths is constant within a small uncertainty, but the relative errors to the individual levels are much larger unless additional information is used. To demonstrate this consistency, if the β feeding to either 0^+ level is completely removed from the MTAS fit, the resulting β-feeding intensity to the remaining 0^+ level is 81.0(5)%. (There are additional uncertainties dominated by the β simulation fidelity that increase the final reported uncertainty to the summed feeding of both 0^+ levels of 81(2)%.)

The 0^+_2 feeding intensity can be isolated by normalizing to the 1024-keV γ-ray intensity, which decays through the 0^+_2 level [21]. The β feedings of these two levels are associated with conversion electrons; therefore it is important to identify when conversion electrons are detected. The conversion electron can be identified in the segmented silicon-strip detectors, where the conversion electrons stand out as a clear peak. The energy spectrum from one of the central silicon strips is shown in Fig. 4.

By gating on the conversion electron peak in each silicon detector and looking at the coincident signal in MTAS, the relative β-decay feeding for events with conversion electrons can be identified. The conversion-electron events include all events with β feedings that decay directly to or through the 0^+_2 level. In this energy gate on the conversion-electron peak, there is a background of regular ^{98}Nb and ^{98}Zr events and variations in normalizing this component are the dominant uncertainty of the 0^+_2 to 1024-keV γ-ray normalization. The relative amount of direct β feeding to the 0^+_2 state compared to feeding to higher lying states that decay through the 0^+_2 level is identified by fitting the resulting conversion-electron gated MTAS energy spectrum with conversion-electron gated response functions. The two main branches that produce conversion electrons are the direct β decay to the 0^+_2 level and the β decay to the 1759-keV level that decays to the 0^+_2 level via a 1024-keV γ ray. The fit of the conversion electron coincident total MTAS energy spectrum, after the coincident MTAS energy spectrum is subtracted, is shown in Fig. 5.

The signal from the 1759-keV level is a single 1024-keV γ ray, the peak of which is identifiable in Fig. 5 (and also in Fig. 3). There is less than 0.6% additional feeding identified through the 735-keV 0^+_2 level beyond the direct 0^+_2 and direct 1759-keV feedings, with the additional feeding limit dominated by low statistics. From the fit shown in Fig. 5, the ratio of the direct 735-keV 0^+_2 level feeding to the 1024-keV γ ray is 4.8(3). The uncertainty in the ratio is dominated by the background subtraction of the full ^{98}Nb energy spectrum from the conversion-electron gated energy in the individual silicon strips. By normalizing the direct 735 keV 0^+_2 β feeding to the total amount of feeding through the 1759-keV level via the 1024-keV γ ray (obtained from the total MTAS fit) the

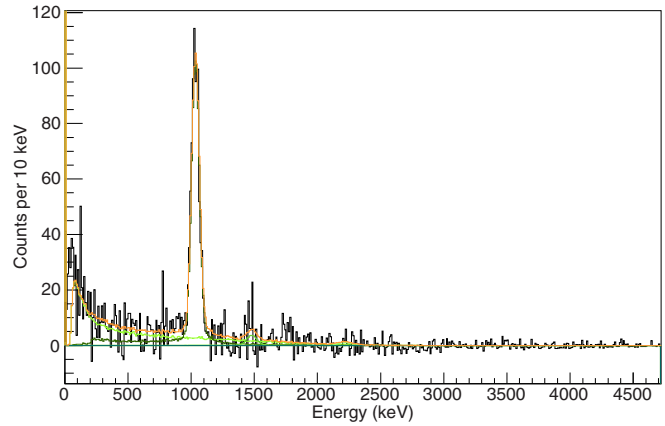

FIG. 5. Fit of MTAS data with a gate on the conversion-electron energy in the β detector. The nonconversion electron background subtracted data (by normalizing on the 787-keV peak) is shown in black, and the various components, colored, and the sum of these components is shown in orange. The 1024-keV peak is from the 1759-keV level that decays via a 1024-keV γ ray and a conversion electron.

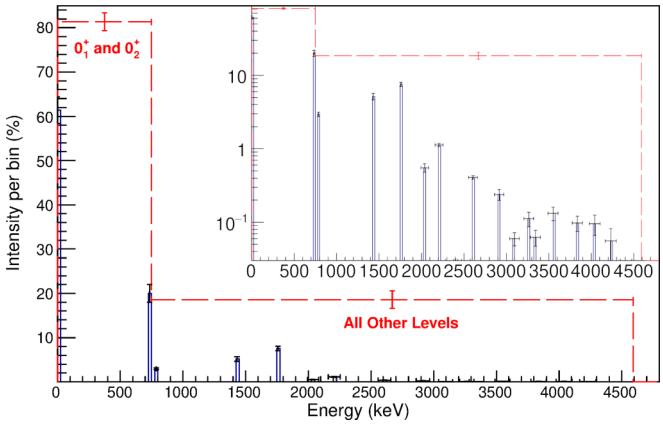

FIG. 6. Comparison of the MTAS level by level feeding β-feeding intensities (solid) to the MTAS summed γ and non-γ β-feeding intensities (dashed). The non-γ β-feeding intensities includes the first two levels, the ground state and the 735-keV level. Both of these levels are 0^+ levels and decay without any associated γ rays. All of the rest of the β feeding includes at least one γ ray in the decay to the ^{98}Mo ground state. The extracted MTAS β-feeding intensities with uncertainties are tabulated in Table I in the Appendix. Inset is a logarithmic plot of the same histograms.

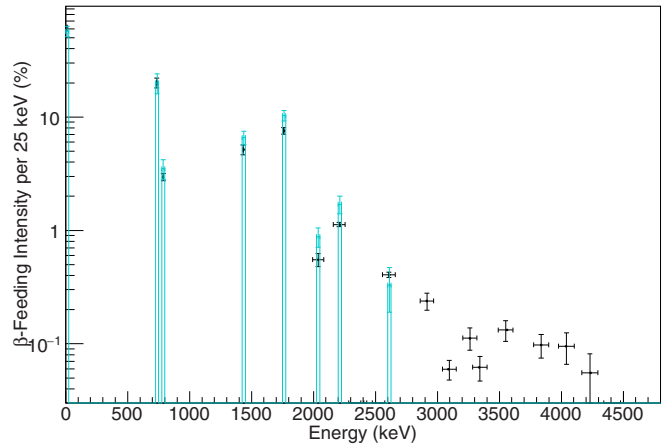

FIG. 7. Comparison of the MTAS (black) and ENSDF (cyan) β-feeding intensities. When comparing the MTAS results with the ENSDF values, the increase of the ground-state feeding lowers the β feeding to the previously known higher energy levels. The MTAS ground-state feeding is 61(3)% and the ENSDF ground-state feeding is 57(6)%. The extracted MTAS β-feeding intensities with uncertainties are tabulated in Table I in the Appendix.

direct amount of β feeding to the 735-keV 0^+_2 β feeding is obtained.

A direct β-feeding intensity to the 735-keV 0^+_2 level of 20(2)% is obtained, while the probability of creating an $E0$ conversion electron from the 735-keV level per ^{98}Nb β decay is 24(2)%. The β-decay feeding to the 0^+_2 level is in agreement with the reported ENSDF value of 20(4)%, but with the reported uncertainty improved by a factor of 2. The extracted probability to create an $E0$ conversion electron from the 735-keV level per ^{98}Nb β decay, 24(2)%, is in agreement with the reported value of 26(6)% [20], but with a reported uncertainty improved by a factor of 3.

VII. MTAS ^{98}Nb β-FEEDING INTENSITIES

The extracted β-feeding intensities are shown in Fig. 6. In Fig. 6, there are two histograms used to represent the ^{98}Nb β-feeding distribution. One histogram groups the β-feeding intensities to the two 0^+ levels in one bin and the β decays to all other levels in the other bin, and the second histogram represents the β-feeding intensities to individual states in ^{98}Mo. The second histogram represents a finer energy binning that distinguishes between the known levels along with the energy uncertainties from newly identified β-decay fed levels. The newly identified β-fed level energies are not precisely identified, nor are the γ multiplicities of the decay from these new levels precisely identifiable due to the low statistics. The latter results in uncertainties on the direct β feeding to these new levels due to the unknown γ multiplicity as these levels de-excite to the ^{98}Mo ground state [28,30]. There are known levels in ^{98}Mo at these higher energies identified via non-β-decay experiments, but which exact level is fed is not clear, since there are often several previously identified low-spin levels within the MTAS energy uncertainty that could be fed via Gamow-Teller β decay.

The dominant uncertainty of the β decays to levels that de-excite with at least one γ ray is the anticorrelated uncertainty with the two 0^+ levels. If the total β feeding to the 0^+ levels is increased from 81% to 83% (1σ), then the total β feeding to the higher energy levels must be decreased, from 19% to 17%, which is about a 10% relative error on all the higher level β feeding. There is a similar uncertainty on the higher β fed levels if the 0^+ levels is decreased from 81% to 79%. This anticorrelated uncertainty of all of the excited states with the two 0^+ levels dominates the uncertainty of the average γ-decay heat.

To extract the direct to ground-state feeding, the extracted 0^+_2 level β feeding, 20(2)%, is subtracted from the measured β feeding to both 0^+ levels, 81(2)%, with the errors added in quadrature. This results in an extracted ground-state feeding of 61(3)%, which represents an improved precision by a factor of 2.

VIII. COMPARISON WITH PREVIOUS MEASUREMENTS

There are several previous measurements of ^{98}Nb β-decay feeding intensities [17–20]. These previous experimental results diverge in reported conversion-electron intensities, in ground-state feeding intensities, and in excited-state β-feeding intensities. Some of the differing results may be attributable to the different source preparation techniques, one group of results based on activation of samples and chemical separation [17–19], and the other on the extraction from fission products [20], and one uses a combination of both techniques [19]. Our results are more in line with the previous fission product experiment [20]. A comparison of the extracted MTAS β-feeding intensities with the ENSDF β-feeding intensities for ^{98}Nb is shown in Fig. 7.

Though in rough agreement, there is a consistent bias when comparing the present results with those of Ref. [20]. Those results [20] are based on the ratio of a γ line from the mass 97 decay chain compared to the intensity of a γ from the mass 98 decay chain. In Ref. [20], the mass 97 γ ray is normalized to the mass 98 γ ray assuming only ^{98}Rb is extracted from the source and the ratio of the two lines is given by the ^{98}Rb neutron emission probability. If there was any appreciable ^{98}Sr extracted from the source, this assumption would not be satisfied. The extraction of only ^{98}Rb and no ^{98}Sr from the source seems unlikely, since the ^{98}Rb fission production plummets by roughly two orders of magnitude relative to ^{98}Sr fission production [26]. In Ref. [20], an upper limit of 5% ^{98}Sr extracted from the source was assumed and was used in the error propagation. Comparison with the MTAS β-feeding data suggests roughly a 15% non-^{98}Rb mass 98 contamination in the [20] source.

The assumed normalization relative to the detected mass 97 chain propagates to β-feeding intensities as a power of the γ multiplicity, and the decay paths from higher energy levels have more γ rays in them. This suggests the reason that the ratio of the MTAS β-feeding intensities to the ENSDF β-feeding intensities gets larger for the higher energy levels when compared with the single 787-keV γ ray line.

The conversion electron per β decay is consistent with [20]. The 734-keV level conversion electron was normalized to the conversion electron from the ^{98}Zr 854-keV level, which is in the 98 mass chain and therefore should not be affected by the possible additional mass 98 nuclei in the source used in Ref. [20].

IX. AVERAGE γ ENERGY PER ^{98}Nb β DECAY

The average γ energy per ^{98}Nb β decay, $\langle E_\gamma \rangle$, is

$$\langle E_\gamma \rangle = \sum_i I_{DPi} E_{\gamma i}, \tag{1}$$

where I_{DPi} is the intensity of the ith decay path and $E_{\gamma i}$ is the energy emitted as one or more γ rays in that decay path. The sum includes the β feeding to the ground state, and even though the γ energy from the ground-state decay path is zero, the uncertainty of the ground-state β-feeding intensity impacts $\langle E_\gamma \rangle$. Other than the $E0$ conversion electron from the 0^+_2 level, the small impact of other conversion electrons is taken into account using the internal conversion electron coefficients given in Refs. [21,31]. The $\langle E_\gamma \rangle$ calculated from the MTAS β-feeding intensities is 275(29) keV. The current ENDF/B-VIII.0 value of the average γ energy per ^{98}Nb β decay is 321(2) keV [2]. Most of the change and uncertainty comes from the increase to the ground-state feeding, which due to anticorrelation with all other states, reduces the excited-state feeding intensities. The increased uncertainty in $\langle E_\gamma \rangle$ dominantly comes from the anticorrelation between the excited states and the ground-state β-feeding intensities. The impact of the uncertainty of the previous ground-state feeding is likely not included in the uncertainty quoted in ENDF/B-VIII.0.

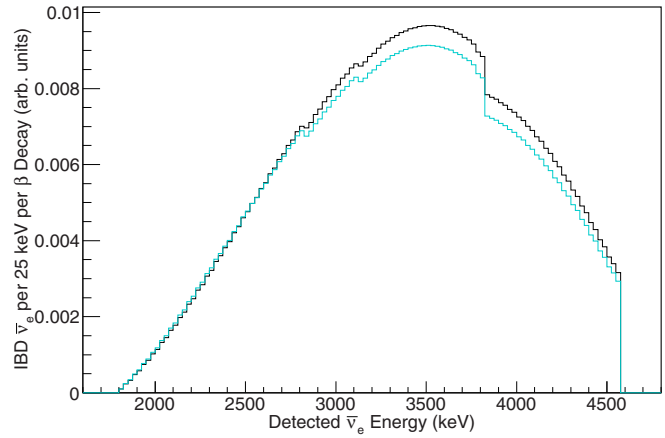

FIG. 8. Comparison of the MTAS (black) and ENSDF (cyan) inverse-β decay events per β decay per energy bin intensities. Most of the change comes from the increased feeding to the ^{98}Mo ground state.

X. REACTOR-$\bar{\nu}_e$ IMPACT

Due to the increase of the ^{98}Nb ground-state β feeding compared with the ENSDF value, the number of high-energy $\bar{\nu}_e$ created increases. This results in an increase in the number of $\bar{\nu}_e$ detected via the inverse-β decay reaction. The number of detected reactor $\bar{\nu}_e$s increases due to the $\bar{\nu}_e$ energy squared dependence of the inverse-β decay cross section and the 1.8-MeV reaction threshold [32]. The detected number of $\bar{\nu}_e$ per energy per ^{98}Nb β decay is shown in Fig. 8. The total number of $\bar{\nu}_e$ detected per ^{98}Nb β decay increases by about 5%. This type of adjustment to the current nuclear data can only be found by direct measurement of ground-state to ground-state feedings, emphasizing the importance of total absorption measurements of major reactor fission products.

The impact of the ^{98}Nb changes on the inverse β decay spectrum by fuel type are shown in Fig. 9. The net result is

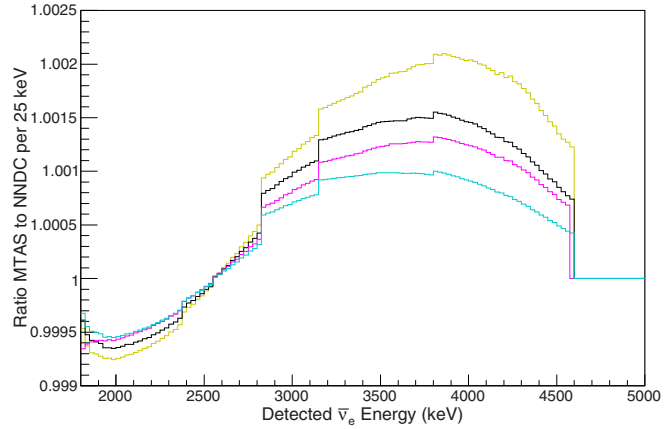

FIG. 9. Ratio of the MTAS to ENSDF inverse-β decay detected per fission by fuel type, ^{235}U (black), ^{238}U (cyan), ^{239}Pu (yellow), and ^{241}Pu (magenta). The only changes considered are from the ^{98}Nb β decay. The net result is an excess due to changes in the ground-state feeding, contrary to the usual reduction from the pandemonium effect.

a 0.1–0.2% increase of inverse β detected $\bar{\nu}_e$s with energies between 3 and 4.6 MeV, depending on the fuel type considered. For a pandemonium-type effect, the usual result is a decrease in the number of inverse β detected $\bar{\nu}_e$s, where here an increase is observed.

^{98}Nb is one of four contributors to a possible discontinuity in the measured $\bar{\nu}_e$ energy spectrum near 4.5 MeV [7]. This discontinuity is due to the end-point energy for several β decays all having approximately the same value. The present results increase the ^{98}Nb $\bar{\nu}_e$ contribution near 4.5 MeV by about 8%when compared with the ENSDF β feeding pattern, thus making the predicted discontinuity in the $\bar{\nu}_e$ energy spectrum larger.

XI. CONCLUSIONS

Even well-studied nuclei located only one β decay away from stability need to have the current β-decay feeding intensities validated using techniques such as total absorption spectroscopy. It is demonstrated that the Modular Total Absorption Spectrometer array is capable of studying the properties of $E0$ decays.

When compared with previous results from ^{98}Nb sources extracted from fission, the reported ground-state feeding increases from 57(6)% to 61(3)%, while the probability to create an $E0$ conversion electrons from the 735-keV level per β decay is slightly reduced from 26(6)% to 24(2)%. The present 0^+_2 β-feeding intensity results are in agreement with the previous results, but the precision is increased by a factor of 3. The feeding to the sum of the first two 0^+ levels is reported as 81(2)%, changed from the ENSDF value of 77(7)%. Again this is in agreement (using the ENSDF uncertainty, σ_{ENSDF}), but the new reported uncertainty is greatly improved. Finally a small amount of additional β feeding, <0.8%, to new levels above the previously highest identified β-populated energy level is reported.

The β-feeding pattern changes lead to a reduction in the average γ energy per ^{98}Nb β decay, $\langle E_\gamma \rangle$, to 275(29) keV. More appropriate uncertainties show the impact of the ground-state feeding precision on $\langle E_\gamma \rangle$. The decrease in $\langle E_\gamma \rangle$ corresponds with an increase in the number of inverse β-decay detected $\bar{\nu}_e$ per ^{98}Nb decay by about 5%. Though the ground-state feeding is in agreement (within $1\sigma_{\text{ENSDF}}$) with the ENSDF value, the reported MTAS ground-state feeding represents a 7% relative increase when compared with the current ENSDF value. This increase to the ground-state β feeding increases the number of largest energy $\bar{\nu}_e$s, which are the most likely to be detected via the inverse β-decay reaction. The increased ground-state feeding also enhances the $\bar{\nu}_e$ energy spectrum fine structure near 4.5 MeV.

The possible impacts on all aspects of reactor-based physics are good reason to study many β-decaying fission products using total absorption spectroscopy. The changes to the ^{98}Nb β-feeding pattern measured with the Modular Total Absorption Spectrometer demonstrate the need to validate and improve the precision of ground-state feeding for nuclei with large cumulatively produced fission products, even ones near stability.

The Department of Energy will provide public access to these results of federally sponsored research in accordance with the DOE Public Access Plan [33].

ACKNOWLEDGMENTS

We would like to thank the ORNL Tandem operations staff for providing the excellent quality proton beams necessary for this work. This research was also sponsored by the Office of Nuclear Physics, U.S. Department of Energy, under Contracts No. DE-AC05-00OR22725 (ORNL), No. DE-FG02-96ER40983 (UTK), No. DE-FG02-96ER40978 (LSU), No. DE-FG02-96ER41006 (MSU), and No. DE-SC0016988 (TTU), and supported by Grant No. UMO-

TABLE I. ^{98}Nb β-feeding intensities, $\mathbf{I}_\beta$. Ratio is the ratio of MTAS I_β to the ENSDF I_β.

Level (keV)	MTAS I_β (%)	MTAS logft[a]	ENSDF I_β (%) [21]	Mach logft ($\sim I_\beta$) [20]	Ratio
0	61(3)	4.693(24)	57(6)	4.7 ($I_\beta \approx 60\%$[b])	1.07(13)
735	20(2)	4.84(5)	20(4)	4.8 ($I_\beta \approx 20\%$[b])	1.0(2)
787	3.0(3)	5.64(5)	3.5(7)	5.6 ($I_\beta \approx 3\%$[b])	0.86(18)
1432	5.2(5)	5.05(5)	6.6(9)	4.5 ($I_\beta \approx 20\%$[b])	0.79(12)
1759	7.6(7)	4.69(5)	10.3(11)		0.74(9)
2038	0.55(7)	5.64(6)	0.88(17)		0.63(15)
2207	1.13(11)	5.20(5)	1.7(3)		0.66(12)
2608	0.4(1)	5.32(11)	0.33(14)		1.2(6)
2915(50)	0.24(4)	5.24(9)	0.0		
3096(50)	0.06(1)	5.65(10)	0.0		
3265(50)	0.11(3)	5.18(14)	0.0		
3343(50)	0.06(2)	5.35(16)	0.0		
3551(50)	0.13(3)	4.71(13)	0.0		
3837(50)	0.10(2)	4.31(14)	0.0		
4041(50)	0.10(3)	3.83(20)	0.0		
4231(50)	0.06(3)	3.4(3)	0.0		

[a]NNDC Logft calculator [34].
[b]NNDC Logft calculator used to estimate I_β with no attempt at uncertainties [34].

2016/23/B/ST2/03559 from the Polish National Centre for Science. This manuscript has been partially supported by Contract No. DE-AC05-00OR22725 with the U.S. Department of Energy and managed by UT-Battelle, LLC. The U.S. Government retains and the publisher, by accepting the article for publication, acknowledges that the U.S. Government retains a nonexclusive, paid-up, irrevocable, world-wide license to publish or reproduce the published form of this manuscript, or allow others to do so, for U.S.Government purposes.

APPENDIX: TABULATED ^{98}Nb β-FEEDING INTENSITIES

The β-feeding intensities from the Modular Total Absorption Spectrometer (MTAS) and previous experiments are summarized in Table I. The ratio is the MTAS I_β divided by the ENSDF I_β. In Ref. [20] only log-ft values with no uncertainties are reported. These log-ft values from Ref. [20] are converted to approximate β-feeding intensities using Ref. [34], assuming allowed β decays.

[1] J. C. Hardy, L. C. Carraz, B. Jonson, and P. G. Hansen, Phys. Lett. B **71**, 307 (1977).
[2] D. Brown, M. Chadwick, R. Capote, A. Kahler, A. Trkov, M. Herman, A. Sonzogni, Y. Danon, A. Carlson, M. Dunn *et al.*, Nucl. Data Sheets **148**, 1 (2018).
[3] T. Yoshida and A. L. Nichols, *Assessment of Fission Product Decay Data for Decay Heat Calculations: A report by the Working Party on International Evaluation Co-operation of the Nuclear Energy Agency Nuclear Science Committee* (Nuclear Energy Agency, Organization for Economic Co-operation and Development, Paris, France, 2007).
[4] A. C. Hayes, J. L. Friar, G. T. Garvey, G. Jungman, and G. Jonkmans, Phys. Rev. Lett. **112**, 202501 (2014).
[5] D. A. Dwyer and T. J. Langford, Phys. Rev. Lett. **114**, 012502 (2015).
[6] A. A. Sonzogni, T. D. Johnson, and E. A. McCutchan, Phys. Rev. C **91**, 011301(R) (2015).
[7] A. A. Sonzogni, M. Nino, and E. A. McCutchan, Phys. Rev. C **98**, 014323 (2018).
[8] R. Greenwood, R. Helmer, M. Putnam, and K. Watts, Nucl. Instrum. Methods Phys. Res., Sect. A **390**, 95 (1997).
[9] M. Karny, L. Batist, B. Brown, D. Cano-Ott, R. Collatz, A. Gadea, R. Grzywacz, A. Guglielmetti, M. Hellström, Z. Hu *et al.*, Nucl. Phys. A **640**, 3 (1998).
[10] A. Algora, D. Jordan, J. L. Tain, B. Rubio, J. Agramunt, A. B. Perez-Cerdan, F. Molina, L. Caballero, E. Nacher, A. Krasznahorkay, M. D. Hunyadi, J. Gulyas, A. Vitez, M. Csatlos, L. Csige, J. Aysto, H. Penttila, I. D. Moore, T. Eronen, A. Jokinen, A. Nieminen, J. Hakala, P. Karvonen, A. Kankainen, A. Saastamoinen, J. Rissanen, T. Kessler, C. Weber, J. Ronkainen, S. Rahaman, V. Elomaa, S. Rinta-Antila, U. Hager, T. Sonoda, K. Burkard, W. Huller, L. Batist, W. Gelletly, A. L. Nichols, T. Yoshida, A. A. Sonzogni, and K. Perajarvi, Phys. Rev. Lett. **105**, 202501 (2010).
[11] A. A. Zakari-Issoufou, M. Fallot, A. Porta, A. Algora, J. L. Tain, E. Valencia, S. Rice, V. Bui, S. Cormon, M. Estienne, J. Agramunt, J. Aysto, M. Bowry, J. A. Briz, R. Caballero-Folch, D. Cano-Ott, A. Cucoanes, V. V. Elomaa, T. Eronen, E. Estevez, G. F. Farrelly, A. R. Garcia, W. Gelletly, M. B. Gomez-Hornillos, V. Gorlychev, J. Hakala, A. Jokinen, M. D. Jordan, A. Kankainen, P. Karvonen, V. S. Kolhinen, F. G. Kondev, T. Martinez, E. Mendoza, F. Molina, I. Moore, A. B. Perez-Cerdan, Z. Podolyak, H. Penttila, P. H. Regan, M. Reponen, J. Rissanen, B. Rubio, T. Shiba, A. A. Sonzogni, C. Weber (IGISOL Collaboration), Phys. Rev. Lett. **115**, 102503 (2015).
[12] B. C. Rasco, M. Wolińska-Cichocka, A. Fijałkowska, K. P. Rykaczewski, M. Karny, R. K. Grzywacz, K. C. Goetz, C. J. Gross, D. W. Stracener, E. F. Zganjar, J. C. Batchelder, J. C. Blackmon, N. T. Brewer, S. Go, B. Heffron, T. King, J. T. Matta, K. Miernik, C. D. Nesaraja, S. V. Paulauskas, M. M. Rajabali, E. H. Wang, J. A. Winger, Y. Xiao, and C. J. Zachary, Phys. Rev. Lett. **117**, 092501 (2016).
[13] A. Fijałkowska, M. Karny, K. P. Rykaczewski, B. C. Rasco, R. Grzywacz, C. J. Gross, M. Wolinska-Cichocka, K. C. Goetz, D. W. Stracener, W. Bielewski, R. Goans, J. H. Hamilton, J. W. Johnson, C. Jost, M. Madurga, K. Miernik, D. Miller, S. W. Padgett, S. V. Paulauskas, A. V. Ramayya, and E. F. Zganjar, Phys. Rev. Lett. **119**, 052503 (2017).
[14] B. C. Rasco, K. P. Rykaczewski, A. Fijalkowska, M. Karny, M. Wolińska-Cichocka, R. K. Grzywacz, C. J. Gross, D. W. Stracener, E. F. Zganjar, J. C. Blackmon, N. T. Brewer, K. C. Goetz, J. W. Johnson, C. U. Jost, J. H. Hamilton, K. Miernik, M. Madurga, D. Miller, S. Padgett, S. V. Paulauskas, A. V. Ramayya, and E. H. Spejewski, Phys. Rev. C **95**, 054328 (2017).
[15] J. Gombas, P. A. DeYoung, A. Spyrou, A. C. Dombos, A. Algora, T. Baumann, B. Crider, J. Engel, T. Ginter, E. Kwan, S. N. Liddick, S. Lyons, F. Naqvi, E. M. Ney, J. Pereira, C. Prokop, W. Ong, S. Quinn, D. P. Scriven, A. Simon, and C. Sumithrarachchi, Phys. Rev. C **103**, 035803 (2021).
[16] A. C. Dombos, A. Spyrou, F. Naqvi, S. J. Quinn, S. N. Liddick, A. Algora, T. Baumann, J. Brett, B. P. Crider, P. A. DeYoung, T. Ginter, J. Gombas, S. Lyons, T. Marketin, P. Möller, W.-J. Ong, A. Palmisano, J. Pereira, C. J. Prokop, P. Sarriguren, D. P. Scriven, A. Simon, M. K. Smith, and S. Valenta, Phys. Rev. C **103**, 025810 (2021).
[17] K. Hubenthal, Comptes Rendus de l'Académie des Sciences, Serie B **264**, 1468 (1967).
[18] B. Fogelberg, Phys. Lett. B **37**, 372 (1971).
[19] W. Herzog, N. Trautmann, R. Denig, and G. Herrmann, Z. Phys. A **276**, 393 (1976).
[20] H. Mach and R. L. Gill, Phys. Rev. C **36**, 2721 (1987).
[21] J. Chen and B. Singh, Nucl. Data Sheets **164**, 1 (2020).
[22] M. Karny, K. P. Rykaczewski, A. Fijałkowska, B. C. Rasco, M. Wolińska-Cichocka, R. K. Grzywacz, K. C. Goetz, D. Miller, and E. F. Zganjar, Nucl. Instrum. Methods Phys. Res., Sect. A **836**, 83 (2016).
[23] M. Wolińska-Cichocka, K. P. Rykaczewski, A. Fijałkowska, M. Karny, R. K. Grzywacz, C. J. Gross, J. W. Johnson, B. C. Rasco, and E. F. Zganjar, Nucl. Data Sheets **120**, 22 (2014).
[24] B. C. Rasco, A. Fijałkowska, M. Karny, K. P. Rykaczewski, M. Wolińska-Cichocka, R. Grzywacz, and K. C. Goetz, Nucl. Instrum. Methods Phys. Res., Sect. A **788**, 137 (2015).
[25] D. Stracener, Nucl. Instrum. Methods Phys. Res., Sect. B **204**, 42 (2003).

[26] J.-I. Katakura, F. Minato, and K. Ohgama, EPJ Web Conf. **111**, 08004 (2016).
[27] P. Shuai *et al.*, Phys. Rev. C **105**, 054312 (2022).
[28] B. C. Rasco, A. Fijałkowska, K. P. Rykaczewski, M. Wolińska-Cichocka, M. Karny, R. K. Grzywacz, K. C. Goetz, C. J. Gross, D. W. Stracener, E. F. Zganjar *et al.*, Acta Phys. Pol. B **48**, 507 (2017).
[29] R. C. Greenwood, R. G. Helmer, M. A. Lee, M. H. Putnam, D. A. Oates, M. A. Struttmann, and K. D. Watts, Nucl. Instrum. Methods Phys. Res., Sect. A **314**, 514 (1992).
[30] B. C. Rasco, A. Fijałkowska, M. Karny, K. Rykaczewski, M. Wolińska-Cichocka, K. C. Goetz, R. K. Grzywacz, C. J. Gross, K. Miernik, and S. V. Paulauskas, JPS Conf. Proc. **6**, 030018 (2015).
[31] T. Kibedi, T. Burrows, M. Trzhaskovskaya, P. Davidson, and C. Nestor, Nucl. Instrum. Methods Phys. Res., Sect. A **589**, 202 (2008).
[32] A. Strumia and F. Vissani, Phys. Lett. B **564**, 42 (2003).
[33] http://energy.gov/downloads/doe-public-access-plan.
[34] https://www.nndc.bnl.gov/logft/.